Rheology of dense granular suspensions: from spheres to fibers

Élisabeth Guazzelli

Aix-Marseille Univ, CNRS, IUSTI, Marseille, France
elisabeth.guazzelli@univ-amu.fr

in collaboration with J. E. Butler, O. Pouliquen, S. Shaikh, F. Tapia.

Non-linear Mechanics and Rheology of Dense Suspensions:
Nanoscale Structure to Macroscopic Behavior
Kavli Institute for Theoretical Physics 2018

Complex mobile particulate systems

used in engineering and found in nature

Lava fountain and flow,
Kilauea, Hawaii (June 7, 1984)

https://volcanoes.usgs.gov

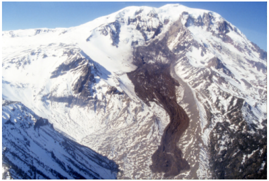

Rock and ice debris avalanche,
Mount Adams (October 20, 1997)

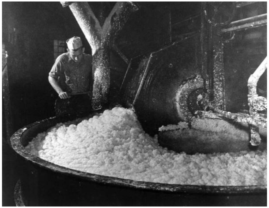

Pulp at a paper mill near Pensacola,
Florida, 1947, from wikipedia

Museum of Civilizations in Europe and the Mediterranean (MuCEM) designed by
Rudy Ricciotti: Ultra-High Performance Fiber-Reinforced concrete (UHPFRC)

1. The suspension as an single effective fluid
   - Suspension viscosity
   - Non-Newtonian behavior: Normal stresses
2. Two-phase flow of suspensions: Particle pressure
3. An alternative frictional approach
4. Toward more complex particulate systems: Rheology of dense fiber suspensions
5. Conclusion

A sheared viscous suspension of non colloidal particles

Suspension of rigid neutrally-buoyant spheres

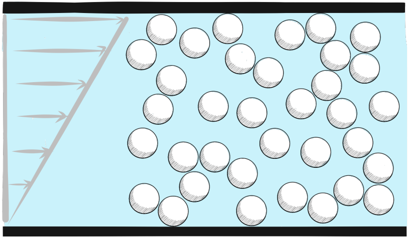

Buoyancy effect

$$\frac{\rho_p - \rho_f}{\rho_f} \to 0$$

Inertial/viscous effects

$$Re_p = \frac{\rho_f a^2 \dot{\gamma}}{\eta_f} \to 0$$

Brownian motion

$$Pe = \frac{6\pi\eta_f \dot{\gamma} a^3}{kT} \to \infty$$

Suspension viscosity

Suspension of rigid, neutrally-buoyant, non-colloidal, mono-disperse, hard spheres
The scaling of the shear stress is viscous: $\tau = \eta_s(\phi)\,\eta_f\dot{\gamma}$ with $\dot{\gamma} = \sqrt{2\,\mathbf{E}:\mathbf{E}}$

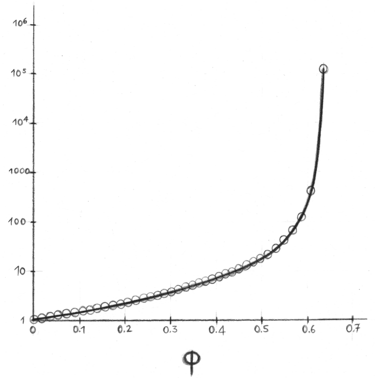

from *A Physical Introduction to Suspension Dynamics*
Guazzelli & Morris (Illustrations by Pic)
Cambridge Texts in Applied Mathematics CUP 2012

Viscosity $O(\phi)$

Einstein 1905

$\eta_s = 1 + 5\phi/2$

First effects of particle interactions

Batchelor & Green 1972

$\eta_s = 1 + \frac{5}{2}\phi + 6.95\phi^2$
for pure straining BUT not for simple shear because closed pair trajectories

Empirical correlation

Krieger 1972

$\eta_s = (1 - \phi/\phi_c)^{-\alpha}$ with $\alpha \approx 2$

Jamming transition

Lerner *et al.* 2012; Andreotti *et al.* 2012; ...

steric/elastic interactions

Relative viscosity of suspensions $\eta_s(\phi)$

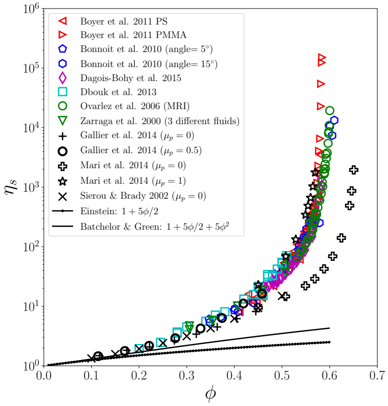

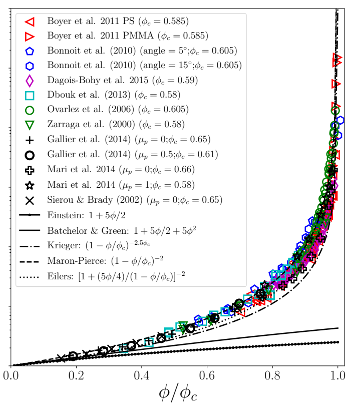

Divergence as $(\phi - \phi_c)^{-2}$ when $\phi \to \phi_c$ with $\phi_c \approx 0.54 - 0.62 < \phi_{crp} \approx 0.64$ $\therefore$ frictional spheres!
Shear-jamming fraction varies depending on size distribution and surface interactions (friction)

Normal stresses in suspensions

Normal stress differences

- $N_1 = \Sigma_{11} - \Sigma_{22}$
- $N_2 = \Sigma_{22} - \Sigma_{33}$

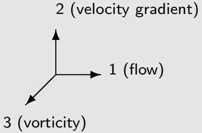

Normal stress differences in non-Brownian suspensions

- $N_1, N_2 \propto \eta_f \dot{\gamma}$ linear in $\dot{\gamma} = \sqrt{2\,\mathbf{E} : \mathbf{E}}$
- $N_i/\tau = O(1) \equiv \alpha_i(\phi)$ same divergence as $\phi \to \phi_c$
- $|N_2| \gg |N_1|$
- N_2 negative but sign of N_1 more elusive!

Gadala-Maria 1979, Zarraga, Hill & Leighton 2000; Singh & Nott 2003; Couturier, Boyer, Pouliquen & Guazzelli 2011; Dai, Bertevas & Tanner 2013; Dbouk, Lobry & Lemaire 2013; Gamonpilas, Morris & Denn 2016
Sierou & Brady 2002; Gallier, Lemaire, Peters & Lobry 2014; Gallier, Lemaire, Lobry & Peters 2016

Normal stress coefficients $\alpha_1 = N_1/\tau$ and $\alpha_2 = N_2/\tau$

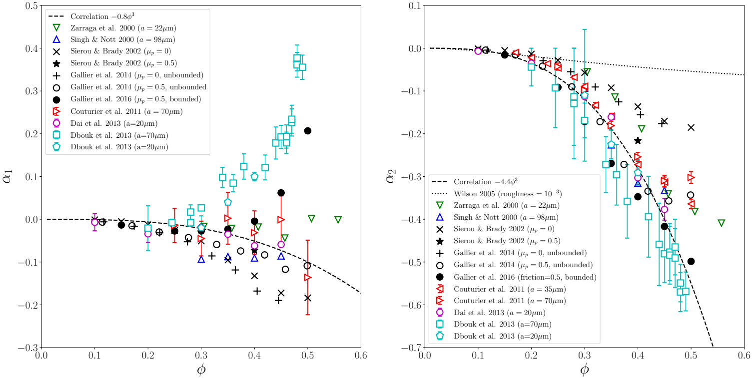

- First normal stress coefficient $\alpha_1(\phi)$ small but sign elusive: negative, positive, or null!
- Second normal stress coefficient $\alpha_2(\phi)$ negative and magnitude increases with increasing ϕ
- Simulations show importance of friction and effect of confinement/walls

Beyond the single-fluid view: Two-phase flow

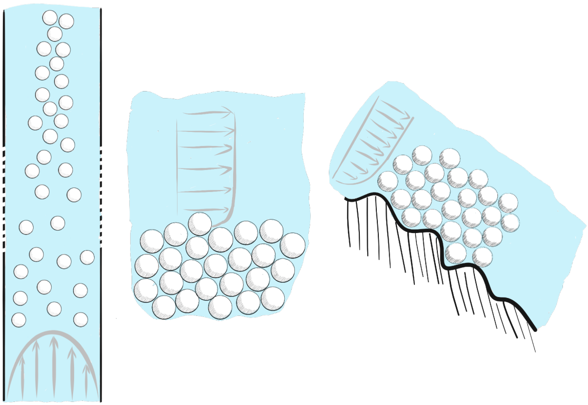

Examples of two-phase suspension flows: (left) Shear-induced migration of neutrally-buoyant spheres in a pressure-driven Poiseuille flow in a tube; (middle) Erosion of sedimented particles under the action of viscous fluid shearing flows; (right) Submarine avalanches forced by the fluid shear stress

Particle pressure in sheared suspension

Suspension mixture incompressible but not particle phase!

Measurement of osmotic pressure

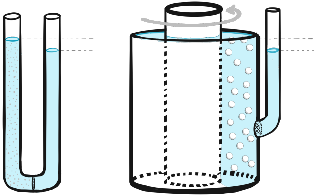

Deboeuf, Gauthier, Martin, Yurkovetsky & Morris 2009

Particle pressure P^p (or more generally particle normal-stress $\boldsymbol{\sigma}^p$)

analogous to the osmotic pressure (or more generally osmotic stress) exerted by both colloidal particles and dissolved molecules

Yurkovetsky & Morris 2009

Normal viscosity

$P^p = \eta_n(\phi)\,\eta_f\,\dot{\gamma}$ viscous scaling

Morris & Boulay 1999

- not often easily captured

  Prasad and Kytömaa 1995; Boyer, Guazzelli & Pouliquen 2011; Garland, Gauthier, Martin & Morris 2013
- crucial for two-phase flow modeling (e.g. modeling shear-induced migration)

Modeling shear-induced migration

Discrete particle simulations

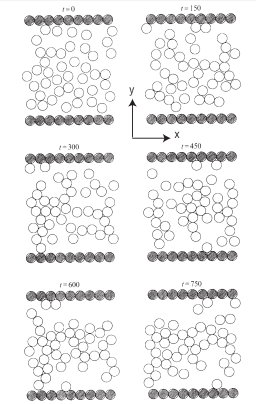

Stokesian Dynamics
Nott & Brady 1994

Suspension balance model (two-phase model)

Particle flux related to the divergence of the particle-phase normal-stress:

$$\mathbf{j}_{\perp} \propto \nabla \cdot \boldsymbol{\sigma}^{p}$$

Nott & Brady 1994; Morris & Boulay 1999; Lhuillier 2009; Nott, Guazzelli & Pouliquen 2011

Correlations for $\boldsymbol{\sigma}^{p}$ required!

e.g. Morris & Boulay 1999; Boyer, Guazzelli & Pouliquen 2011

Simple 2D fully-developed pipe flow

- Steady fully developed flow in the x-direction with variation of properties in the y-direction
- Particle y-momentum balance
  $\frac{\partial P^{p}}{\partial y} = \frac{\partial[\eta_{n,2}(\phi)\,\dot{\gamma}(y)]}{\partial y} = 0$
- Where the shear rate is low, the concentration is high and vice versa

Shear-induced migration in oscillatory pipe flow

Concentration profile in pipe flow and comparison with the SBM using the rheology of Morris & Boulay 1999 and Boyer, Guazzelli & Pouliquen 2011

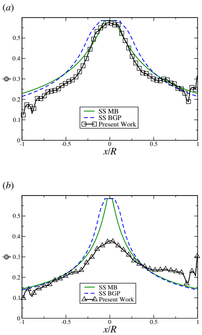

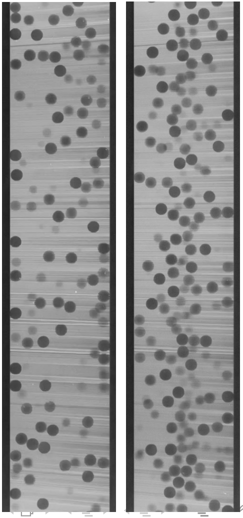

At smaller ϕ_0, SBM fails to predict that the steady concentration at the center of the pipe falls below that of $\phi_c \approx 0.585$

Good agreement of SBM and experiments at large ϕ_0 but some discrepancies at smaller ϕ_0 and for the dynamics

Snook, Butler & Guazzelli 2016

Volume-imposed versus pressure-imposed rheometry

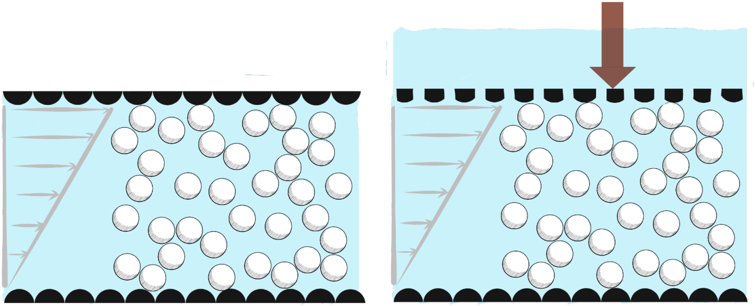

Volume-imposed rheometry:
$P^p, \tau, \dot{\gamma}, \phi, \eta_f$

- $\tau = \eta_s(\phi)\,\eta_f\dot{\gamma}$
- $P^p = \eta_n(\phi)\,\eta_f\dot{\gamma}$

Viscous scaling of the stresses

Pressure-imposed rheometry:
$\phi, \tau, \dot{\gamma}, P^p, \eta_f$

- $\tau / P^p = \mu(J)$
- $\phi = \phi(J)$

$J = \eta_f \dot{\gamma}/P$ **viscous** dimensionless shear rate

Pressure-imposed rheology of suspension

Alternative frictional view coming from the rheology of dry granular materials

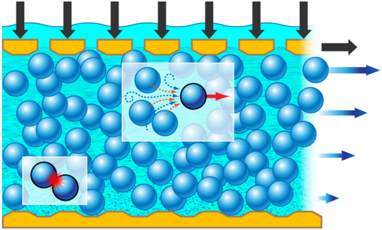

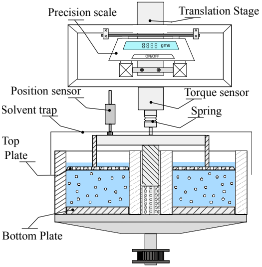

- Top porous plate enabling fluid to flow through it but not particles
- Simultaneous measurements of ϕ, $\dot{\gamma}$, τ, $P^p (\equiv -\sigma^p_{22}$ here)

- Examination of the rheology close to the jamming transition
- Measurements of the particle pressure P^p

Boyer, Guazzelli & Pouliquen 2011

Unifying P-imposed and ϕ-imposed rheologies

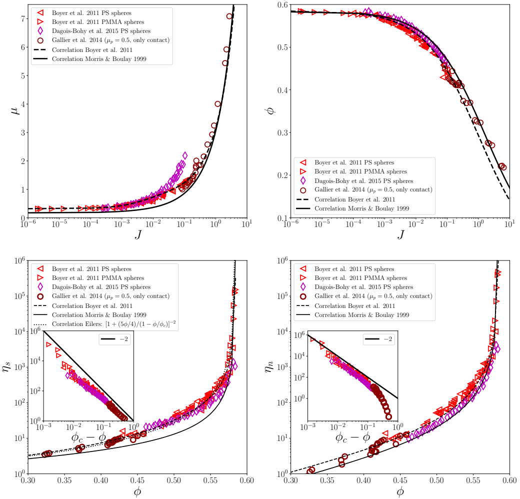

Classical effective viscosity recovered from frictional view

$\mu = \tau / P^p = \eta_s / \eta_n$

$J = \eta_f \dot{\gamma} / P^p = 1/\eta_n$

$\therefore$

$\eta_s = \mu / J$

$\eta_n = 1/J$

at vanishing J:

$\mu_c \approx 0.30 - 0.32$

$\phi_c \approx 0.58 - 0.59$

η_s and η_n diverge as $(\phi_c - \phi)^{-2}$

Rheology of rigid fiber suspensions

The different regimes of fiber suspensions

The dilute ($n \ll 1/L^3$), semi-dilute ($1/L^3 \lesssim n \ll 1/L^2 d$), concentrated ($n \gtrsim 1/L^2 d$) regimes and ordered nematic state ($n \gg 1/L^2 d$)

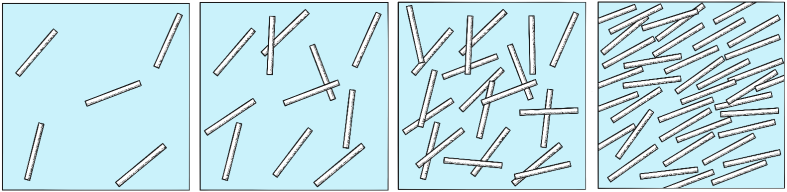

Rheology of viscous Newtonian fluids containing rigid fibers relatively unexplored

- Yield stresses and nonlinear scaling of τ with $\dot{\gamma}$ (shear-thinning)
  Ganani & Powell 1985; Powel 1991
- Rheological studies at relatively small ϕ ($\phi \lesssim 0.17$ for $A = 17 - 18$; $\phi \lesssim 0.23$ for $A = 9$)
  Bibbó 1985; Bounoua, Lemaire, Férec, Ausias & Kuzhir 2016

ϕ- and P-imposed rheometry of dense fiber suspensions

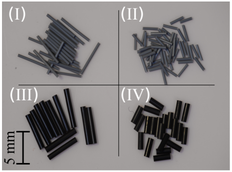

Rigid fibers with different aspect ratios

Fiber label	Symbol	A
(I)	□	14.5 ± 0.8
(II)	△	6.3 ± 0.4
(III)	◊	7.2 ± 0.4
(IV)	◯	3.4 ± 0.3

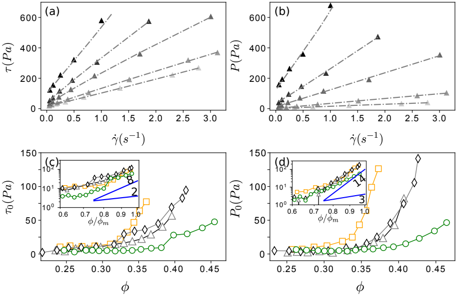

Viscous scaling: τ and P linear in $\dot{\gamma}$
But **non-zero yield-stresses**, τ_0 and P_0, at $\dot{\gamma} = 0$

- τ_0 and P_0 increase with ϕ, more sharply for higher A
- Origin of yield stresses still remains unknown

Rheological data after subtracting apparent yield-stresses

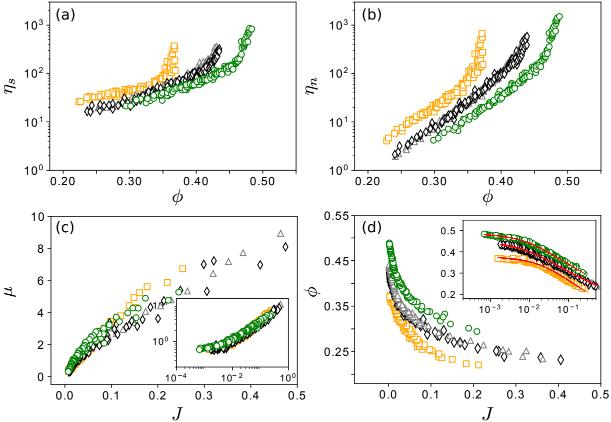

- $\eta_s = (\tau - \tau_0)/\eta_f \dot{\gamma}$ and $\eta_n = (P - P_0)/\eta_f \dot{\gamma}$ increase with ϕ and diverge at $\phi_c(A)$ with shift towards lower values of ϕ with increasing A
- ϕ decreasing function of J with shift towards lower values of ϕ with increasing A
- Complete collapse of all data for $\mu(J)$ $\therefore$ μ independent of A

Critical values at jamming

Comparisons with:

- Experiments of Rahli, Tadrist & Blanc 1999 (■) on the dry packing of rigid fibers
- Simulations of Williams & Philipse 2003 (▲) for the maximum random packing of spherocylinders
- Data (★) obtained by Boyer, Guazzelli & Pouliquen 2011 for suspensions of spheres ($A = 1$)

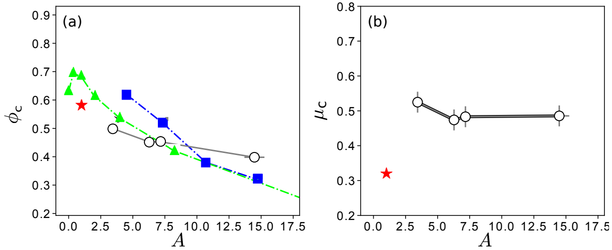

- ϕ_c decreases with increasing A such as for dry packing; organized structure for $A = 15$?
- At jamming, $\mu_c \approx 0.47$ (larger than value ≈ 0.32 for spheres) independent of A

Scaling at the jamming transition

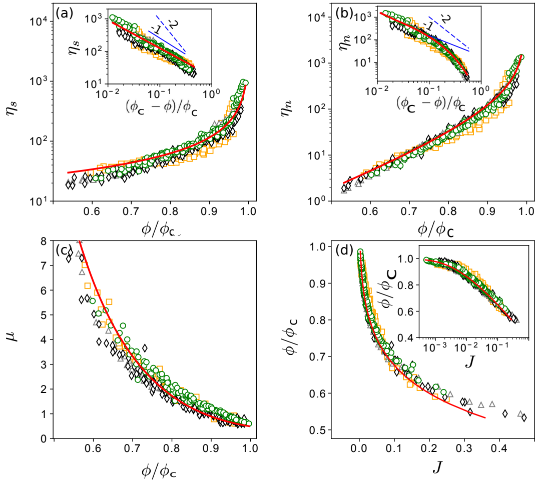

Tapia, Shaikh, Butler, Pouliquen & Guazzelli 2017

Scaling

Good collapse of all the data by rescaling by $\phi_c(A)$

η_s and η_n diverge as $\approx (\phi_c - \phi)^{-1}$

Constitutive laws

$$\mu(\phi) = \mu_c + \alpha \left(\frac{\phi_c - \phi}{\phi}\right) + \beta \left(\frac{\phi_c - \phi}{\phi}\right)^2$$

with $\mu_c = 0.47$, $\alpha = 2.44$, and $\beta = 10.20$

$$\eta_s(\phi) = 14.51 \left(\frac{\phi_c - \phi}{\phi_c}\right)^{-0.90}$$

$$\eta_n(\phi) = \eta_s(\phi)/\mu(\phi)$$

1. The suspension as an single effective fluid
   - Suspension viscosity
   - Non-Newtonian behavior: Normal stresses

2. Two-phase flow of suspensions: Particle pressure

3. An alternative frictional approach

4. Toward more complex particulate systems: Rheology of dense fiber suspensions

5. **Conclusion**

Conclusions

Rheology of dense granular suspensions

Mainly controlled by the contact interactions between particles

Pressure-imposed rheology of suspensions of non-colloidal hard spheres

- Rheology close to the jamming transition: η_s and η_n diverge as $\sim (\phi_c - \phi)^{-2}$
- Measurements of particle pressure

Pressure-imposed rheology of dense suspensions of non-colloidal hard fibers

- Subtracting apparent yield-stresses (adhesive forces? transient jamming?) reveals a viscous scaling for both the shear and normal stresses.
- η_s and η_n diverge as $\sim (\phi_c - \phi)^{-1}$ with $\phi_c(A)$ and μ independent of A
- Organized microstructure? Link between rheology and microstructure?

And also normal stress differences and migration in fiber suspensions

Snook, Davidson, Butler, Pouliquen, Guazzelli 2014; Strednak, Shaikh, Butler, Guazzelli 2018 in preparation